

# Photorefractive dynamic optical interconnects

Shimon Weiss, Mordechai Segev, Shmuel Sternklar, and Baruch Fischer

We present and demonstrate a set of dynamic optical interconnects which are based on the double phase conjugate mirror with photorefractive wave mixing. These devices are bidirectional, self-adjusting, and controllable in real time. Uses in various interconnection modes are given.

## I. Introduction: Optical Interconnects and Photorefractive Devices

Photonics-based technology is expected to influence significantly the fields of communication, information processing, and computing. Further substantial developments depend on progress in new concepts and technology of light beam manipulation and control. This will lead to better basic devices, such as optical switches, interconnects, deflectors, valves, and spatial light modulators (SLMs). The addressing mechanism of such devices may be electronic in a hybrid electrooptic system or optical in an all-optical processor.

An interconnection device, illustrated in Fig. 1, connects an optical input vector (or matrix)  $I$  to an optical output vector (or matrix)  $O$ . The input vector may be provided by a 1- or 2-D array of sources of fibers, lasers, SLMs etc. The output vector is usually an array of fibers or detectors. In two-way, or bidirectional, links the two vectors have the same role. Each vector element represents a station, or a terminal, consisting of a transmitter and receiver. Several modes of operation are described in Fig. 2: broadcasting [Fig. 2(a)]; combining [Fig. 2(b)], point to point [Fig. 2(c)], and crossbar switching [Fig. 2(d)] operations. Many structures and implementations of optical interconnects can be found in Refs. 1–3. The devices are all-optical or hybrid electrooptical, and the media in which the optical signals are to be linked can be free space, optical fibers, and integrated optical waveguides. Several ways of free-space interconnects have been proposed. The holographic lens, for example, which consists of

fixed diffraction gratings at each node,<sup>4,5</sup> lacks the desired reconfiguration and switching property, and is also very sensitive to optical misalignments. The crossbar switch can be implemented by a 2-D SLM (electrooptic or all-optic) or by an all-optical switching array.<sup>6,7</sup> Another suggestion is the use of dynamic four-wave mixing for writing a real-time holographic lens. This system, consisting of arrays of beam steering gratings,<sup>6</sup> is reconfigurable and incorporates both steering and switching properties.

Photorefractive (PR) materials excel in providing efficient interaction of light beams even in very moderate power densities of a few mW/mm<sup>2</sup>. Such low intensities are compatible with semiconductor lasers. In PR crystals such as BaTiO<sub>3</sub>, Bi<sub>12</sub>SiO<sub>20</sub>, (BSO), Sr<sub>1-x</sub>Ba<sub>x</sub>Nb<sub>2</sub>O<sub>6</sub> (SBN), and GaAs, spatially varying light intensities induce refractive-index variations. As a result multibeam interference patterns produce gratings which are the means for the beams' interaction. The very efficient beam coupling process in some of the crystals, mainly due to their large electrooptic coefficient, has led to many novel devices, such as several phase conjugators and photorefractive oscillators.<sup>8</sup> Here we will concentrate in one of these oscillators, the double phase conjugate mirror (DPCM).<sup>9</sup>

In the DPCM, shown in Fig. 3(b), two input light beams denoted by 2 and 4 with amplitudes  $A_i$  enter the opposite sides of a photorefractive crystal. For beam coupling strengths higher than a threshold value, a four-wave mixing process builds up,<sup>9</sup> in which two other beams 1 and 3 emerge from the crystal without any external feedback to the PR interaction region. Such feedback was needed in all other PR oscillators. The two input beams 2 and 4 need not be mutually coherent and can be derived from separate lasers.<sup>9</sup> In the DPCM all beams have degenerate wavelengths, and the output beams 1 and 3, which are derived from the inputs 4 and 2, respectively, have the following phase conjugate relationship:  $A_1 \propto A_2^*$  and  $A_3 \propto A_4^*$ . In the four-wave mixing process each of the two input

The authors are with Technion—Israel Institute of Technology, Department of Electrical Engineering, Haifa 32000, Israel.

Received 3 November 1987.

0003-6935/88/163422-07\$02.00/0.

© 1988 Optical Society of America.

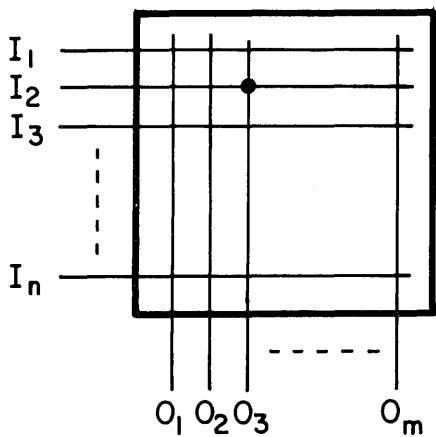


Fig. 1. General interconnecting device links the input vector  $I$  to the output vector  $O$ . An interconnected node is shown by a full dot, as for  $I_2O_2$  in the figure.

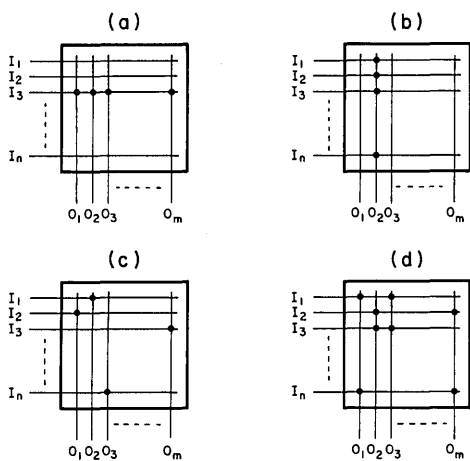


Fig. 2. Various interconnect configurations: (a) broadcasting; (b) combining; (c) point to point; (d) crossbar switch.

beams interferes and photorefractively writes a grating with a portion of its self-diffracted output beam (beam 4 with 1 and 2 with 3). This permits coupling of incoherent input beams and oscillation even in slowly responding crystals. Moreover, we recently demonstrated the operation of a similar oscillator, the double color pumped oscillator (DCPO), with two inputs of different colors.<sup>10</sup> In this device the output beams have an angular offset with respect to the input beams and do not have the exact phase conjugation relationship of the DPCM. A variety of applications have been suggested and demonstrated with these oscillators. Among them are bidirectional spatial light modulation, image edge enhancement, thresholding,<sup>11</sup> beam cleanup, multilaser coupling and locking,<sup>9</sup> image color conversion, and light beam steering.<sup>10</sup>

The bidirectional phase conjugation capability of the DPCM motivated our suggestion<sup>11</sup> and other recent works<sup>12,13</sup> to use it as a real-time two-way information link between 2-D matrix ports. Its basic feature is similar to conventional holographic devices. The ad-

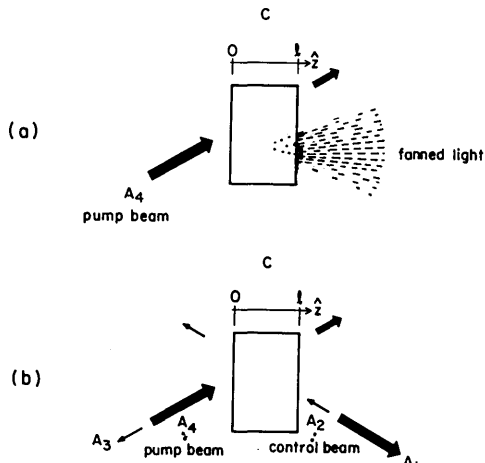


Fig. 3. Double phase conjugate mirror as an optical switch: (a) off position: the PR crystal  $C$  is pumped by one (or no) strong light beam  $A_4$ . This beam is scattered in a wide angle (the fanning effect); (b) on position: directing a second control beam  $A_2$  to the opposite side of the crystal results in the collapse of the fanned light into two oscillating beams,  $A_1$  and  $A_3$  in antiparallel directions (phase conjugation) with respect to the two input beams.

vantages of the real-time operation and the active and addressable controlling capabilities make the DPCM much more attractive. The additional steering property of the double color DCPO<sup>10</sup> allows an extra degree of freedom in dynamically controlling the beams. Other PR interconnect schemes have been suggested in Ref. 14.

We present various configurations of optical interconnects which are based on the PR DPCM. These dynamic interconnection devices are all-optical, bidirectional, and programmable in real time and have self-adjusting capabilities.

In Sec. II we review the operation of the DPCM. Section III describes broadcasting interconnection scheme. Sections IV and V deal with point-to-point links based on time division multiplexing and wavelength division multiplexing, respectively, and thereafter concluding remarks are given.

## II. The DPCM as an Optical Switch

The DPCM can be used as an optical switch and a beam steerer, as described in Fig. 3. In the off position the photorefractive crystal is pumped by one (or no) light beam ( $A_4$  in the figure). This beam is scattered in a wide angle (the fanning effect). The link is on when the two beams,  $A_2$  and  $A_4$ , are simultaneously directed to the opposite sides of the crystal. This results in the collapse of the fanned light into two oscillating beams,  $A_1$  and  $A_3$ , in antiparallel directions (phase conjugation) with respect to the two input beams. While the two input beams exchange their spatial structures, the photons and their temporal (intensity and average phase) information are transmitted through the DPCM, namely,  $A_1$  and  $A_3$  carry the temporal information  $A_4$  and  $A_2$ , respectively.

The symmetry of the DPCM with respect to the two input beams permits its possible use for bidirectional

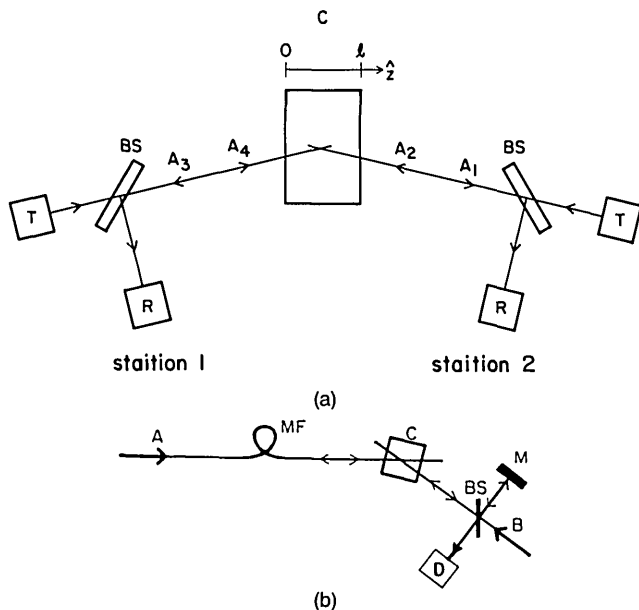


Fig. 4. (a) Bidirectional transmitting-receiving scheme: *C*, crystal; *T*, transmitter; *R*, receiver; *BS*, beam splitter. (b) Wave front matching for coherent detection by interfering the signal beam *A*, which was distorted by the multimode fiber *MF*: *M*, mirror; *D*, detector or screen.

communication link between two stations. This requires that the transmitter and receiver of a given station use the same unit. The transmitted information retraces, in a phase conjugate manner, the counterpropagating input beam. Care must be taken to prevent the injection of light into the transmitter to avoid undesirable noise and injection locking effects. Bidirectional transmitting-receiving stations are illustrated in Fig. 4(a).

The typical slow time response of PR crystals (orders of seconds for BaTiO<sub>3</sub> with mW/mm<sup>2</sup> light intensities and approximately inversely proportional to the light intensity<sup>8</sup>) relaxes the strict need of simultaneous pumping. After the gratings have been built up, the link is on, and a high frequency phase or intensity modulation will not erase the gratings or turn off the link. Therefore, in most situations the link will be held on even without a dc bias of the two input beams 2 and 4. For very low rates, which are much less than the inverse of the crystal time response, the grating erasure will dictate a dc bias to keep the link open. The upper limit of the modulation rate is not limited and is dictated by the detectors and electronics. Fast modulation broadens and changes the effective frequency of the signal beam. This has a similar effect of deflection of the output beam as in the DCPO. Thus the high bit rate detected signals will have a broader beam spot size. Quantitative values can be derived from the results for the DCPO, which is given in Eq. (5). It gives a signal angular spreading of ~0.002 mrad for a 10-GHz modulation rate, which is much less than the diffraction limit of a typical DPCM.

An extra bonus which the DPCM's phase conjugation property provides is its immediate ability to be used for coherent detection. Signal *A* in Fig. 4(b), of which the wavefront was distorted by the multimode fiber, is automatically matched to be interfered with the local beam *B*. We have applied this idea in the past for beam cleanup<sup>9</sup> and interferometry.<sup>15</sup>

According to the analysis in Ref. 9, the transmissivity of the device (neglecting absorption) is symmetric and is given by

$$T = \frac{I_1(l)}{I_4(o)} = \frac{I_3(o)}{I_2(l)} = \frac{a^2(q^{-1/2} + q^{1/2})^2 - (q^{-1/2} - q^{1/2})^2}{4}, \quad (1)$$

where *o* and *l* indicate the two input and output surfaces of the PR crystal and  $I_i = A_i A_i^*$ , *a* is related to the coupling coefficient  $\gamma$  (of the wave mixing process) by

$$\tanh\left(-\frac{\gamma l a}{2}\right) = a, \quad (2)$$

*l* is the beams' interaction length in the crystal and *q* is the input beam ratio, defined by

$$q \equiv \frac{I_4(o)}{I_2(l)}.$$

Equation (2) gives a threshold  $\gamma l$  value,  $|(\gamma l)_t| = 2$ , for the mixing process. Maximum transmission is predicted for  $a \approx 1$  (for high  $\gamma l$ ) and is approximately 1. The range for *q* is

$$\frac{1-a}{1+a} < q < \frac{1+a}{1-a}. \quad (3)$$

The coupling constant  $\gamma$  depends on the various crystal parameters and on the beams' geometry: The relevant electrooptical coefficients, the grating wavelength and orientation (through the beams angles), and the magnitude of the space charge field in the crystal. This dictates some angular bandwidth limitations on the mixing process.<sup>8</sup>

The insertion loss (IL) of the switch is (in decibels)

$$IL = 10 \log \left( \frac{I_4(o)}{I_1(l)} \right) = -10 \log T. \quad (4)$$

Of course, absorption and Fresnel reflections must be included (through the expression of *T*).

The steering capability of the DCPO can provide another dynamic switching technique. This is obtained by wavelength tuning of one of the input beams, causing a controllable deflection of the output beams. The angular deflection outside the crystal is given by<sup>10</sup>

$$d\theta = \alpha d\lambda / \lambda, \quad (5)$$

where  $\alpha$  depends on the geometry of the device. In our experiments  $\alpha = 0.12$ , and the deflection is ~0.25 mrad for a wavelength tuning of 1 nm. Direct control of the PR crystal can provide a few other switching possibilities by affecting the coupling constant  $\gamma$ . Applied electric fields on the crystal, for example, can be used for very rapid on-off operation by changing the polarization state (and hence  $\gamma$ ) of the PR crystal.<sup>16</sup> Another way is the background illumination of the mixing crystal by coherent or incoherent light beams.<sup>17,18</sup>

These techniques may be used for a limited number of links in one crystal according to the separate addressable pixels in the crystal.

### III. Broadcasting

In the previous section we considered only one link between two stations. Here we assume a vector of  $n$  stations imaged into the crystal from one side and a single station from the other side (Fig. 5). This configuration matches Figs. 2(a) and (b), the broadcasting (splitting) or combining mode. It is a DPCM structure, where one pump beam carries a pictorial information (the  $n$ -stations vector). Efficient coupling occurs by slightly focusing the beams in the crystal. However, to obtain equal splitting of the broadcasted signal to the  $n$  receiving stations, the geometry of the mixing must be considered. We assume that all  $n$  stations transmit equal control beams ( $I_2$ ). By dividing the space in the PR crystal for the broadcasted signal  $I_4$  between all the receiving control beams, as illustrated in Fig. 5, it is possible to ensure that the interaction lengths, coupling coefficients, and input beam ratios will be the same for the different interaction regions. According to Eqs. (1) and (2), this will give equal transmissions and splittings.

To establish a communication link in the above scheme, the stations which are about to receive the broadcast have to transmit (information or dc signal) to keep an open line in a kind of hand-shaking communication protocol. By switching the appropriate beams on and off, different values can be assigned to the vectors. In this sense, the device is acting as a dynamic splitter—the broadcasted signal is split and transmitted only to selected stations. Thus the interconnects can be reconfigured in real time—limited by the time response of the crystal. Since this time response is relatively slow, as discussed above, it imposes only a lower limit (of the order of hertz) on the modulation frequency of the signals.

We have carried out an experimental demonstration of the configuration as illustrated in Fig. 6. The input and output vectors (as defined in Fig. 1) were fibers, carrying the light of the 488-nm line of an argon-ion laser, operating in a multilongitudinal mode. The input vector  $\mathbf{I}$  consisted of a single element (fiber) and the output vector  $\mathbf{O}$  of two fibers. We stress that the terms input or output are merely used for convenience purposes, but both vectors have the same role. Each element of the vectors is a station capable of transmitting and receiving.  $\mathbf{O}$  was imaged (with a scale of 1:1) by lens  $L_2$  (focal length  $f = 50$  mm) onto the midplane of the PR BaTiO<sub>3</sub> crystal ( $7 \times 6 \times 3$  mm<sup>3</sup>,  $c$  axis along the 7-mm side). The fibers were 1 mm apart. The light emerging from the single fiber was loosely focused into the crystal in the way suggested in Fig. 5. All the fibers were multimode with a 50- $\mu$ m core. No attempts were made to control the polarization of the light which traversed the fibers. Two beam splitters were positioned between the lenses and the fibers to monitor the phase conjugate outputs. We have measured insertion losses of the device of  $\sim 3$  dB (without accounting for losses of the beam splitters).

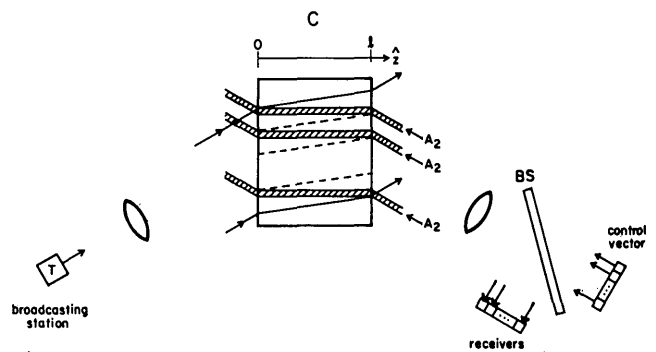


Fig. 5. Implementation of the broadcasting scheme. The control vector and broadcasting station are slightly focused or imaged into the crystal. The imaging optics is not shown.

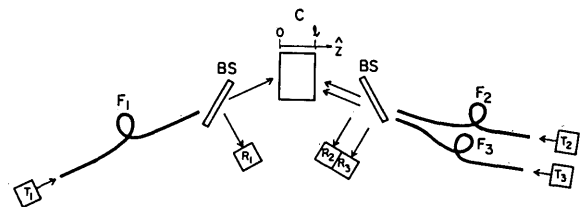


Fig. 6. Experimental configuration with the DPCM for the various interconnections in the paper. The beams guided in the fibers  $F_i$  have as follows: in the broadcasting scheme, the same wavelength of 488 nm; in the point-to-point scheme, 488 and 514.5 nm in  $F_2$  and  $F_3$ , respectively, and each of these two wavelengths in turn in  $F_1$ . In the WDM scheme, 488 and 514.5 nm in  $F_2$  and  $F_3$ , respectively, and the strongest five argon-ion laser lines (simultaneously) in  $F_1$ .

The three beams were modulated by choppers with different frequencies. The phase conjugate signals, taken at the appropriate detectors, are seen in Figs. 7(a) and (b). In Fig. 7(a)  $T_3 = 0$  while in Fig. 7(b)  $T_2 = 0$ . Phase modulation of the signals is also possible. In fact, we have carried such a phase modulation transmission with the DPCM in a former interferometric experiment.<sup>14</sup> It is clear from the figure that no signal crosstalk is present: two temporal signals can traverse the device without interfering. Of course, if  $T_3$  and  $T_2$  were allowed to transmit simultaneously,  $R_1$  would have detected a combination of the two signals. A similar experiment of temporal modulation of two-port DPCM was demonstrated recently.<sup>13</sup>

### IV. Point-to-Point Interconnects

The broadcasting scheme discussed above can be used for point-to-point links by letting only one element of the vector  $\mathbf{O}$  to assume a nonzero value at a given time slot. In such a time division multiplexing (TDM), any interconnect  $I_1O_j$  ( $1 < j < n$ ) can be obtained. This scheme has one drawback: the destined station has to transmit while receiving a message (a dc signal or information) for the DPCM to operate. This imposes constraints on the communication protocol. A more desirable scheme will incorporate self-routing of the messages. This can be done by assigning different wavelengths to the elements of the vector  $\mathbf{O}$  and a tunable laser to  $I_1$ , as illustrated in Fig. 8.

The experimental demonstration was similar to the former one (Figs. 6 and 7) but with beams of different color. Fibers  $F_2$  and  $F_3$  were carrying the 488- and

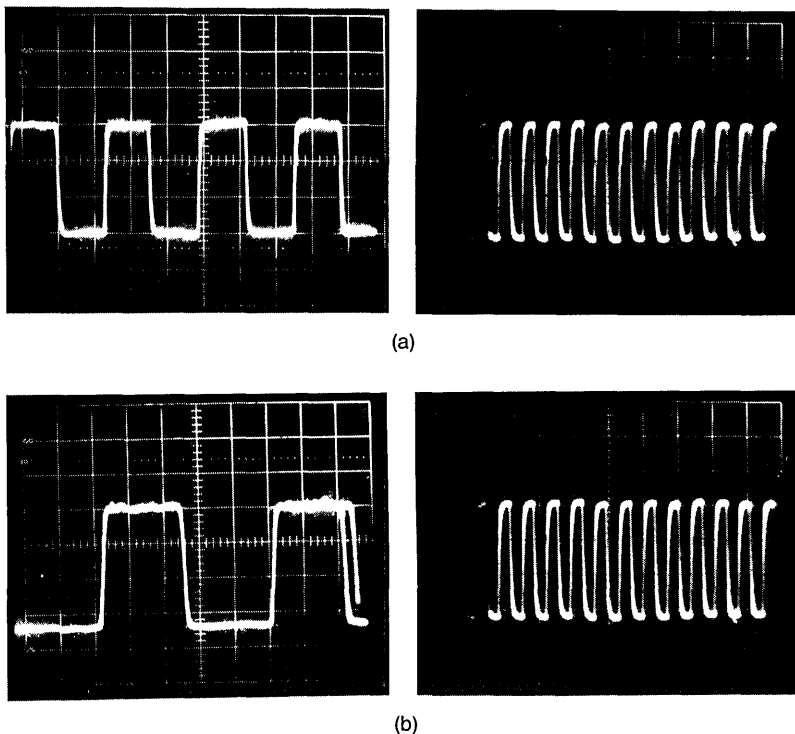


Fig. 7. Optical signals in the experimental configuration of Fig. 6: (a) signals picked up by  $R_1$  (left) and  $R_2$  (right) for  $T_3 = 0$ ; (b) signals picked up by  $R_1$  (left) and  $R_3$  (right) for  $T_2 = 0$  (one division equals 5 ms).

514.5-nm lines of the argon laser, respectively.  $F_1$  was carrying each of these lines in turn. The interaction between beams with the same color produced the phase conjugating output beams in the DPCM manner, establishing a link between them. The cross color interaction was usually not strong enough to compete and to build up a DCPO type oscillation but only typical diffraction cones.<sup>9,10</sup> These cross color diffractions have an angular offset with respect to the input beams,<sup>11</sup> so that undesired crosstalk between different colors will be limited. Yet the diffraction efficiency in this case is lower with respect to the previous scheme due to additional gratings which compete for the PR gain.

The last two schemes described point-to-point interconnects of one element of  $I$  to all elements of  $O$ . By space division multiplexing (SDM), as shown in Fig. 9, it is possible to realize point-to-point links between all the stations of the two vectors, as described in Fig. 2(c). Each of the elements of the input vector  $I$  is imaged (by cylindric lens) to a matrix row (thus being able to broadcast to all the elements of the output vector  $O$ ), and each of the  $O$  elements is imaged to a column. This in practice is a vector-matrix multiplier suggested in Ref. 19. It divides the crystal into  $n \times n$  small volumes; each belong to a single interconnect  $I_i O_j$ . Incorporating TDM to this geometry, where only one element of each vector is allowed to transmit in a given time slot will result in the desired scheme. Again, the protocol has to manage the stations in an efficient policy by avoiding collisions and wasted slots. Another point-to-point scheme utilizing wavelength division multiplexing (WDM) is discussed in the next section.

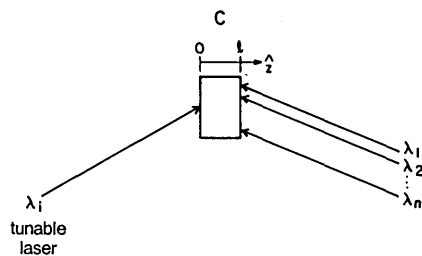


Fig. 8. Point-to-point interconnects. The beam from the left-hand side of the crystal  $C$  with a tunable wavelength  $\lambda_i$  can be linked and tuned to any of the wavelengths  $\lambda_1, \lambda_2, \dots, \lambda_n$  of beams from the right-hand side.

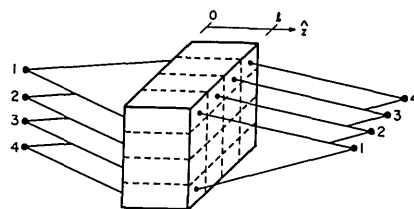


Fig. 9. Space division multiplexing: the two vectors which are interconnected are orthogonally imaged into the crystal creating  $n \times n$  ( $4 \times 4$  in the figure) nodes, each for a single interconnect.

In all the schemes discussed above, reconfigurable interconnects were done by assigning varying values to the two input vectors. Active switching, through the matrix itself, is needed for the realization of a crossbar switch. This can be done by controlling the coupling coefficient  $\gamma$  of each volume element of the crystal of Fig. 9. Selectively erasing the gratings of chosen ma-

trix elements by incoherent light beams<sup>17,18</sup> will result in the desired switching operation. All the stations of the two vectors have to transmit constantly. Interconnects which are to be operative will experience no erasure, while the other matrix element gratings will be erased. Light from SLM 2-D laser or LED arrays, which are imaged into the crystal, such that each of their elements will control a matrix element, can serve as the control unit for the switching.

## V. Wavelength Division Multiplexing

Wavelength division multiplexing (WDM) is described in Fig. 10. In this technique each source has a different wavelength. All the sources are mixed (multiplexed) and coupled to a single channel (fiber). At the end of this channel the different wavelengths are separated (decoded) and picked up by the receivers.<sup>20</sup> This scheme enables the transmission of a very wide bandwidth on a single channel without the time constraints imposed by TDM. Reconfigurable interconnects can also be achieved by tuning the wavelengths of the different sources.

A demonstration of a multiplexer and decoder, with the DPCM, was done with the same experimental configuration illustrated in Fig. 6. We coupled the 488- and 514.5-nm lines into the fibers representing  $O_1$  and  $O_2$ . A beam composed of all five lines of the argon-ion laser was injected into the single fiber representing  $I_1$ . Two dominant sets of gratings developed in the crystal (written by the 488- and 514.5-nm lines), which decomposed the all-lines combination into the 488-nm and 514.5-nm lines (for the light traversing from left to right) and simultaneously combined the two wavelengths, traveling from right to left, into the single fiber. This device is both multiplexer and decoder, depending on the light propagation direction. In this scheme we also noticed nonefficient cross-colored beam interaction manifested in cones of light in an angular offset with respect to the interacting input beams. Thus crosstalk is not a problem, but the diffraction efficiency decreases.

Figure 11(a) displays a bidirectional WDM communication link composed of two DPCMs. When free-space communication is considered, a single-crystal WDM device can be configured as indicated in Fig. 11(b). Further studies should be carried out to investigate the feasible number of channels, the optimum wavelength spacing between adjacent channels, crosstalk, and insertion loss.

## VI. Conclusions

We have presented implementations of optical interconnects by utilizing the double phase conjugate mirror. Broadcasting, point-to-point, and crossbar switch schemes have been demonstrated. The implementation is based on dynamic holography in PR crystal. The self-built and self-Bragg matched gratings of the DPCM allow reconfiguration in real time and ease of stringent alignment constraints. High diffraction efficiencies are due to the oscillatory behavior of the gratings. (The diffracted beam enhances the grating

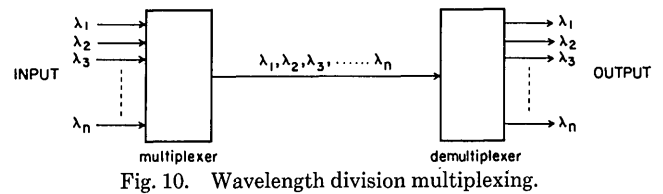


Fig. 10. Wavelength division multiplexing.

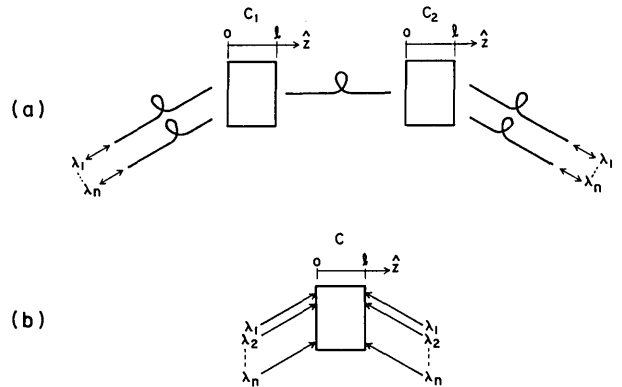


Fig. 11. (a) Wavelength division multiplexing with two DPCMs; (b) wavelength division multiplexing with one DPCM.

which it reads.) The main drawback of the BaTiO<sub>3</sub> crystal is its slow time response, which limits the switching time. The cross-color beam interaction (DCPO type) was shown to be nonproblematic. Careful use of this effect can even provide another means to the dynamic control by the beam steering capability.

This work was supported by the Foundation for Research in Electronics, Computers and Communications, Administrated by the Israel Academy of Sciences and Humanities.

## References

1. May 87 special issue of the IEEE Commun. Mag.
2. Oct. 86 special issue of Opt. Eng.
3. A. A. Sawchuk and T. C. Strand, "Digital Optical Computing," Proc. IEEE 72, 758 (1984); "Optical Crossbar Network," Computer 50 (1987).
4. J. W. Goodman, F. I. Leonberger, S. Y. King, and R. A. Athale, "Optical Interconnections for VLSI Systems," Proc. IEEE 72, 850 (1984).
5. L. A. Bergman, *et al.*, "Holographic Optical Interconnects for VLSI," Opt. Eng. 25, 1109 (1986).
6. J. A. Neff, "Major Initiatives for Optical Computing," Opt. Eng. 26, 003 (1987).
7. E. Marom and N. Konforti, "Programmable Optical Interconnects," Proc. Soc. Photo-Opt. Instrum. Eng. 700, 209 (1986).
8. M. Cronin Golomb, B. Fischer, J. O. White, and A. Yariv, "Theory and Applications of Four Wave Mixing in Photorefractive Media," IEEE J. Quantum Electron. QE-20, 12 (1984); J. O. White, M. Cronin-Golomb, B. Fischer, and A. Yariv, "Coherent Oscillation by Self-Induced Gratings in the Photorefractive Crystal BaTiO<sub>3</sub>," Appl. Phys. Lett. 40, 450 (1982).
9. S. Weiss, S. Sternklar, and B. Fischer, "Double Phase Conjugate Mirror: Analysis, Demonstration and Applications," Opt. Lett. 12, 114 (1985); S. Sternklar, S. Weiss, M. Segev, and B. Fischer, "Beam Coupling and Locking of Lasers Using Photorefractive Four-Wave Mixing," Opt. Lett. 11, 528 (1986).

10. B. Fischer and S. Sternklar, "Self Bragg Matched Beam Steering Using the Double Color Pumped Photorefractive Oscillator," *Appl. Phys. Lett.* **51**, 74 (1987); S. Sternklar and B. Fischer, "Double-Color-Pumped Photorefractive Four Wave Mixing Oscillator and Image Color Conversion," *Opt. Lett.* **12**, 711 (1987).
  11. S. Sternklar, S. Weiss, and B. Fischer, "Optical Information Processing with the Double Phase Conjugate Mirror," *Opt. Eng.* **26**, 423 (1987); B. Fischer, S. Weiss, and S. Sternklar, "Spatial Light Modulation and Filtering Effects in Photorefractive Wave-Mixing," *Appl. Phys. Lett.* **50**, 483 (1987).
  12. M. Cronin-Golomb, A. M. Biernacki, H. Kong, and C. Lin, "Programmable Optical Interconnection Using a Double Phase Conjugate Mirror," *J. Opt. Soc. Am. A* **4**(13), p12 (1987).
  13. H. J. Caulfield, J. Shamir, and Q. He, "Flexible Two-Way Optical Interconnects in Layered Computers," *Appl. Opt.* **26**, 2291 (1987); Q. He, J. G. Duthie, J. Shamir, and H. J. Caulfield, "Optical Parallel Communication with Photorefractive Materials," in *Technical Digest, Topical Meeting on Photorefractive Materials, Effects, and Devices* (Optical Society of America, Washington, DC, 1987).
  14. G. Pauliat and G. Roosen, "Large Scale Interconnections Using Dynamic Gratings," *Proc. Soc. Photo-Opt. Instrum. Eng.* **700**, 202 (1986).
  15. S. Sternklar, S. Weiss, M. Segev, and B. Fischer, "Mach-Zehnder Interferometer with Multimode Fibers Using the Double Phase Conjugate Mirror," *Appl. Opt.* **25**, 4518 (1986).
  16. D. M. Gookin, "Optical Switch Using the Photorefractive Effect and Ferroelectric Polarization Reversal," *Opt. Lett.* **12**, 196 (1987).
  17. Y. Fainman, C. C. Guest, and S. H. Lee, "Optical Digital Logic Operations by Two-Beam Coupling in Photorefractive Material," *Appl. Opt.* **25**, 1598 (1986).
  18. Y. Shi, D. Psaltis, A. Marrakchi, and A. R. Tanguay, Jr., "Photorefractive Incoherent-To-Coherent Optical Converter," *Appl. Opt.* **22**, 3665 (1983).
  19. J. W. Goodman, A. R. Dias, and L. M. Woody, "Fully Parallel, High-Speed Incoherent Optical Method for Performing Discrete Fourier Transforms," *Opt. Lett.* **2**, 1 (1978).
  20. See, for example, H. D. Hendricks, "Wavelength Division Multiplexing," *Proc. Soc. Photo-Opt. Instrum. Eng.* **512**, 130 (1984).
- 

## MEASUREMENT OF LASER OUTPUT CHARACTERISTICS

Effective use of lasers in technology, manufacturing, defense and energy research requires a precise control of the laser output: spatial, spectral, temporal, energy and power. Ability to specify and/or reliably measure these characteristics with a predictable degree of accuracy is a necessity for those working in laser research, development, manufacture, sales, testing and use. Demonstrations and simulated problem sessions are features to reinforce lecture principles, practice calculations and familiarize the student with laser/optics detection equipment and techniques.

ENGINEERING TECHNOLOGY INSTITUTE  
 P.O. Box 8859  
 Waco, TX 76714-8859  
 (817) 772-0082  
 1-800-367-4238

5 Days  
 Cost: \$910.00

October 31–November 4, 1988  
 Albuquerque, NM